Photofragment emission yield spectroscopy of acetylene in the D 1 u , 1 A, and F 1 u + states by vacuum ultraviolet and infrared vacuum ultraviolet double-resonance laser excitations

Mitsuhiko Kono, Kennosuke Hoshina, and Kaoru Yamanouchi

Citation: The Journal of Chemical Physics **117**, 1040 (2002); doi: 10.1063/1.1485064
View online: http://dx.doi.org/10.1063/1.1485064
View Table of Contents: http://scitation.aip.org/content/aip/journal/jcp/117/3?ver=pdfcov
Published by the AIP Publishing

Photofragment emission yield spectroscopy of acetylene in the $\tilde{D}\,^1\Pi_u$, $\tilde{E}\,^1A$, and $\tilde{F}\,^1\Sigma_u^+$ states by vacuum ultraviolet and infrared vacuum ultraviolet double-resonance laser excitations

Mitsuhiko Kono,[a] Kennosuke Hoshina, and Kaoru Yamanouchi[b]
Department of Chemistry, School of Science, The University of Tokyo, 7-3-1 Hongo, Bunkyo-ku, Tokyo 113-0033, Japan

(Received 11 March 2002; accepted 22 April 2002)

The excitation spectra of the $\tilde{D}\,^1\Pi_u$, $\tilde{E}\,^1A$, and $\tilde{F}\,^1\Sigma_u^+$ states of C_2H_2 in the 135.3–130.8 nm range are measured under jet-cooled conditions by detecting fluorescence emitted from $C_2H(\tilde{A}\,^2\Pi)$ or $C_2H(\tilde{B}\,^2A')$ photofragments. In the photofragment emission yield spectra, the origin bands of the $\tilde{D}-\tilde{X}$ and $\tilde{F}-\tilde{X}$ transitions are observed with Lorentzian profiles with bandwidth (Γ) of 58.9(4) and 66.7(2) cm^{-1}, respectively. By identifying the bending progressions of the $\tilde{E}-\tilde{X}$ transition appearing with narrower Lorentzian profiles with, $\Gamma\sim 40\ cm^{-1}$, the band previously considered to be the origin band of the $\tilde{E}-\tilde{X}$ transition is assigned to the transition to the second overtone ($v_3=3$) level in the near-*cis* bending (ν_3) mode. The transitions to the C–H stretch excited levels in the $\tilde{D}$ and $\tilde{F}$ states are observed using the infrared-VUV double resonance excitation scheme. The $\tilde{D}\ 3_1^1$, $\tilde{D}\ 1_1^1\ 3_1^1$, $\tilde{F}\ 3_1^1$, and $\tilde{F}\ 1_1^1\ 3_1^1$ bands are identified at 74 334(3), 74 121(5), 74 522(3), and 74 388(3) cm^{-1}, respectively, with much broader bandwidth ($\Gamma>100\ cm^{-1}$) than the $\tilde{D}-\tilde{X}$ and $\tilde{F}-\tilde{X}$ origin bands, indicating that the dissociation is accelerated significantly in both of the $\tilde{D}$ and $\tilde{F}$ states when the antisymmetric C–H stretch (ν_3) mode in the $\tilde{D}$ and $\tilde{F}$ states is excited. © *2002 American Institute of Physics.* [DOI: 10.1063/1.1485064]

I. INTRODUCTION

Molecular Rydberg states undergo complex bond-breaking processes originating from their mixing with other Rydberg states as well as with nearby valence states. Among small polyatomic molecules, the Rydberg states of acetylene (C_2H_2) have been characterized relatively well by the recent laser spectroscopic studies. It has been known that the electronic transitions to the two Rydberg states, $\tilde{D}$ and $\tilde{F}$, and one valence $\tilde{E}$ state overlap with each other in the vacuum ultraviolet (VUV) wavelength region of 135–130 nm. The $\tilde{D}\,^1\Pi_u$ ($1\pi_u\rightarrow 3d\sigma_g$R) and $\tilde{F}\,^1\Sigma_u^+$ ($1\pi_u\rightarrow 3d\pi_g$R) states are members of the Rydberg states which converge on the electronic ground state of $C_2H_2^+(\tilde{X}\,^2\Pi_u)$ having a linear equilibrium geometry. Therefore, their equilibrium geometries are expected to be linear.[1–9] On the other hand, the $\tilde{E}\,^1A$ state is known to have near-*cis* equilibrium geometry with C_2 symmetry.[10]

In spite of the previous spectroscopic efforts,[1–16] only fragmentary information has been obtained regarding the photodissociation mechanism through this Rydberg-valence complex composed of the $\tilde{D}$, $\tilde{E}$, and $\tilde{F}$ states. Suto and Lee[1] measured using a synchrotron radiation light source an absorption spectrum of C_2H_2 in this VUV wavelength region as well as an excitation spectrum monitoring the yields of the C_2H photofragments produced in the $\tilde{A}\,^2\Pi$ and $\tilde{B}\,^2\Sigma^+$ states, but the measurements were done at room temperature and the resolution of the spectrum was not sufficiently high to resolve the individual line shape of the overlapping vibronic bands in the $\tilde{D}-\tilde{X}$, $\tilde{F}-\tilde{X}$, and $\tilde{E}-\tilde{X}$ transitions. Later, Löffler *et al.*[11,12] measured the kinetic energy profiles of photofragment hydrogen atoms in the 133–121 nm range and identified two competing dissociation pathways which form, respectively, the C_2H fragments in the $\tilde{X}\,^2\Sigma^+$ and $\tilde{A}\,^2\Pi$ states. Considering the complex vibronic structure composed of the three overlapping band systems, it would be an important step to resolve these vibronic bands and derive their rate of dissociation from the respective vibrational levels for understanding the dissociation mechanisms.

In the investigation of the photodissociation through such electronically highly exited states, measurements of a high-resolution excitation spectrum using a tunable VUV laser light source is most promising especially when molecules are prepared at ultralow temperature under jet-cooled conditions. As has been demonstrated for the photodissociation process of OCS via the $2\,^1\Sigma^+$ state, the high-resolving power of the method enables us to discuss absorption peak profiles characteristic of molecules which dissociate in an ultrashort time scale.[17]

In the present study, photodissociation processes of C_2H_2 via the three electronic states, $\tilde{D}$, $\tilde{E}$, and $\tilde{F}$, i.e.,

[a]Present address: Research School of Physical Sciences and Engineering, Australian National University, Canberra, ACT 0200, Australia.
[b]Author to whom correspondence should be addressed.

$$C_2H_2(\tilde{D},\tilde{E},\tilde{F}) \rightarrow C_2H(\tilde{A},\tilde{B}) + H, \quad (1)$$

are investigated by recording an excitation spectrum of C_2H_2 under jet-cooled conditions by using a tunable VUV laser light source. The excitation spectra recorded in the present study are those called photofragment emission yield (PHOFREY) spectra and IR-VUV double-resonance (DR) PHOFREY spectra via the ν_1'' and $\nu_1''+\nu_3''$ levels, in which the yield of the visible fluorescence emitted from the C_2H photofragments in their $\tilde{A}$ and $\tilde{B}$ states[18–26] are monitored. Through a band-shape analysis of these PHOFREY spectra, we investigate (i) how the electronic configuration and the geometrical structure effect the photodissociation process in the energetically closely spaced $\tilde{D}$, $\tilde{E}$, and $\tilde{F}$ electronic states, and (ii) how the vibrational excitation accelerate or decelerate the dissociation depending on the excited vibrational mode.[27–29]

II. EXPERIMENT

A pure acetylene gas with the stagnation pressure of ~2 atm was expanded through a pulsed valve with 0.2 mm orifice diameter (General Valve 9-279-900) into the vacuum chamber to form a pulsed supersonic free jet. The background pressure in the vacuum chamber was kept $<10^{-4}$ Torr. The vacuum pumping system of the chamber was the same as that described previously.[30] The rotational temperature of C_2H_2 in the free jet was estimated to be ~5 K by measuring laser induced fluorescence (LIF) spectra of the $\tilde{A}-\tilde{X}$ transition of C_2H_2 under the same jet-cooled conditions.[31] The collimated VUV beam was introduced into the main vacuum chamber and crossed the free jet at right angles, 15 mm downstream from the orifice of the pulsed valve. In the IR-VUV double resonance experiment, the collimated IR beam was counterpropagated colinearly with the VUV beam. At the laser beam-jet interaction region, the diameters of IR and VUV beams were ~5 and 2 mm, respectively.

Tunable VUV laser light with the wavelength region of $\lambda=130.8-135.3$ nm was used to excite C_2H_2 to the $\tilde{D}$, $\tilde{E}$, and $\tilde{F}$ states. The apparatus used to generate the coherent, tunable VUV light was described previously.[30] Briefly, the VUV laser light was generated by a four-wave difference frequency mixing $(2\omega_1-\omega_2)$ technique in a Kr gas (15–70 Torr) using two dye lasers (Lambda Physik FL2002 for ω_1 and Questek PDL-3 for ω_2) pumped by a XeCl excimer laser (Lambda Physik LPX-105i). The wavelength $\lambda_1=2\pi/\omega_1$ of the second harmonics of the dye laser output generated by a BBO (β-BaB_2O_4) crystal was $\lambda_1=212.56$ nm, which was in two-photon resonant with $Kr\,5p[1/2]_0$, and the wavelength $\lambda_2=2\pi/\omega_2$ generated by the other dye laser was varied between 500 and 580 nm, resulting in the VUV wavelength of $\lambda_{VUV}=130.8-135.3$ nm. When measuring the excitation spectra, the VUV intensity was monitored simultaneously by a photomultiplier tube (Hamamatsu R1259). The ω_1 and ω_2 laser beams were separated from the VUV laser beam by a 30° lithium fluoride prism. Three light buffles were placed between the prism and the main chamber in order to eliminate the visible (ω_2) and UV (ω_1) scattered light in the chamber. The spectral bandwidth of the VUV light was estimated to be ~0.4 cm^{-1} by the peak width of the rotational transitions in the LIF spectrum of the $A-X$ (7, 0) band of CO.

The tunable IR laser output of an optical parametric oscillator and amplifier (OPO/OPA) laser (Continuum Mirage 3000) pumped by an injection-seeded Nd:YAG laser (Continuum Powerlite 8000) was used to prepare C_2H_2 in its specific rotational levels of the ν_3'' ($\lambda=3.03$ μm) and $\nu_1''+\nu_3''$ ($\lambda=1.52$ μm) vibrational states. The fundamental ($\lambda=1064$ nm) and frequency-doubled ($\lambda=532$ nm) outputs of the Nd:YAG laser were introduced into the IR laser which consists of one OPO crystal and two OPA crystal pairs. The output pulse energy of the signal radiation from the first OPA was typically 25 mJ/pulse at ~0.8 μm. This signal beam was frequency-doubled in a KDP crystal and led to a wavemeter (Burleigh WA-5500) to monitor the wavelength. On the other hand, the idler radiation from the first OPA is guided to the second OPA crystal pair and used as an oscillator. The output energies of the signal and idler radiation from the second OPA were typically 15 mJ/pulse at ~1.5 μm and 4 mJ/pulse at ~3 μm, respectively. These two mid-IR beams were separated from each other by a 45° anhydrous-quartz prism.

The wavelength of the signal or idler radiation of the second OPA signal was locked on a rotational line of the vibrational band of C_2H_2 by monitoring the photo-acoustic spectrum. The spectral linewidth of the IR radiation was estimated to be 0.07 cm^{-1} from the IR-VUV double-resonance excitation spectra obtained by scanning the wavelength of the IR light.

The visible fluorescence from the C_2H ($\tilde{A},\tilde{B}$) fragments produced by the photolysis of C_2H_2 in the VUV region was detected by a photomultiplier tube (Hamamatsu R928) through a light collection lens pair located in the direction perpendicular to both the laser beams and the free jet. The signal from the photomultiplier tube was preamplified and averaged by a boxcar integrator (Stanford SR250), and was sent to a personal computer through an analog/digital converter.

III. RESULTS AND DISCUSSION

A. Assignment of the $\tilde{D}$, $\tilde{F}$, and $\tilde{E}$ states

In the upper and lower panels of Fig. 1, the observed PHOFREY spectra in the 73 950–75 350 cm^{-1} and 75 400–76 800 cm^{-1} regions are shown, respectively. The transition wave numbers of the peaks in the PHOFREY spectra are in good agreement with those reported previously.[1,6] No transition to the bend excited levels was identified in either of the $\tilde{D}-\tilde{X}$ or $\tilde{F}-\tilde{X}$ bands, suggesting that the equilibrium geometrical structures of the $\tilde{D}$ and $\tilde{F}$ states are linear as previously inferred.[1–9]

On the other hand, weak but distinctive progressions were identified in the $\tilde{E}-\tilde{X}$ band. This indicates that the $\tilde{E}$ state has a nonlinear equilibrium structure, which is supported by the previous study by Lundberg *et al.*[10] who identified the evidence of a nonplanar, noncentrosymmetric structure of the $\tilde{E}$ state in their rotationally resolved UV–UV double resonance spectra.

In the $\tilde{X}\,^1\Sigma_g^+$, $\tilde{D}\,^1\Pi_u$, and $\tilde{F}\,^1\Sigma_u^+$ states whose equilibrium structure is linear, the normal modes are: ν_1 (C–H symmetric stretch), ν_2 (C–C stretch), ν_3 (C–H antisymmetric stretch), ν_4 (*trans*-bend), and ν_5 (*cis*-bend). In the nonplanar $\tilde{E}\,^1A$ state, the normal modes are the ν_1 (C–H symmetric stretch), ν_2 (C–C stretch), ν_3 (near *cis*-bend), ν_4(torsion), ν_5 (C–H antisymmetric stretch), ν_6 (near-*trans* bend).[10] It should be noted that the classification as well as the numbering of the normal modes for the $\tilde{E}$ state with C_2 symmetry is different from those in the $\tilde{X}$, $\tilde{D}$, and $\tilde{F}$ states with $D_{\infty h}$ symmetry.

Regarding the assignment of the origin of the $\tilde{E}-\tilde{X}$ band, consensus has not been reached yet. Herman and Colin assigned the band observed at 74 629 cm^{-1} to the origin of the $\tilde{E}-\tilde{X}$ band,[6] which corresponds to the peak appearing in our PHOFREY spectrum at 74 615 cm^{-1}. The same assignment was adopted later by Lundberg *et al.*[10] On the other hand, Ashfold *et al.* assigned the transitions at 74 629 cm^{-1} to the $3\nu_3'$ band (ν_3': C–H antisymmetric stretch).[14] When 74 615 cm^{-1} is adopted as the origin of the $\tilde{E}-\tilde{X}$ band, the bands observed at ~74 029 and ~75 011 cm^{-1} need to be assigned as hot-band transitions from the *trans*-bend excited level in the $\tilde{X}$ state. However, under jet-cooled conditions hot-bands are not expected to appear with such strong intensities. Therefore, it may not be appropriate to regard the band at 74 615 cm^{-1} as the $\tilde{E}-\tilde{X}$ origin band.

When adopting the peak at 72 753 (Ref. 14), 72 746 (Ref. 15) or 72 744 (Ref. 16) cm^{-1} as the origin band transition, the peak at 74 615 cm^{-1} in the present study can be assigned to the $\tilde{E}$ $(3\nu_3')$ band (ν_3': near *cis*bend), and other unassigned peaks in Fig. 1 can be interpreted straightforwardly as members in the two progressions, $\tilde{E}$ $(n\nu_3')$ $(n=2-5)$ and $\tilde{E}$ $(\nu_2'+n\nu_3')$ $(n=1-3)$ with respect to the ν_3' mode. The vibrational assignments for the transitions to the $\tilde{D}$, $\tilde{E}$, and $\tilde{F}$ states are shown in Fig. 1, where the $\tilde{F}$ $(n'\nu_3')\leftarrow\tilde{X}$ $(n''\nu_3'')$ transition is denoted as $\tilde{F}\,3_{n''}^{n'}$, for example.

The peak positions of the $\tilde{E}-\tilde{X}$ bands appearing in our PHOFREY spectrum are in good agreement with those in the two-photon resonance multiphoton ionization spectra recorded by Ashfold *et al.*[14] and Takahashi *et al.*[15] These two groups interpreted the vibrational progression as that of the $^1\Delta_g$ Rydberg $(1\pi_u\rightarrow 3p\pi_u R)$ state. However, the transition to the $^1\Delta_g$ Rydberg state should be symmetrically forbidden in the one-photon absorption scheme as far as the equilibrium structure is linear. Therefore, the agreement between the one-photon and the two-photon transitions can be regarded as an evidence that the $\tilde{E}$ state has a nonlinear equilibrium structure. The $\tilde{E}\,^1A$ valence state with a near-*cis* C_2 symmetry is possibly formed by the interaction between the $^1\Delta_g$ $(1\pi_u\rightarrow 3p\pi_u R)$ Rydberg state and the $^1\Sigma_u^+(1\pi_u\rightarrow 1\pi_g)$ valence state because both of these two electronic states are expected to be located around the wavelength region investigated in the present study.[5,9]

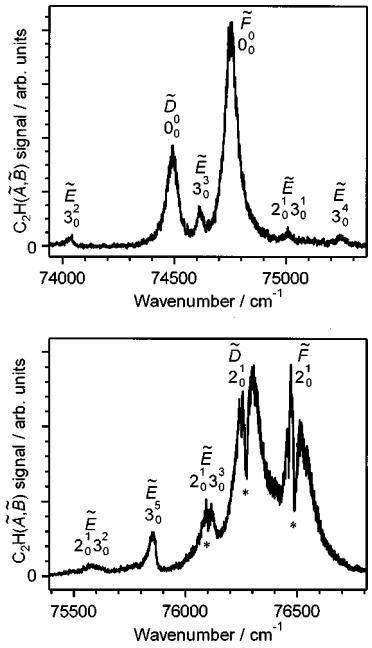

FIG. 1. The PHOFREY spectrum of C_2H_2 in the 73 950–76 800 cm^{-1} range recorded by monitoring the fluorescence emitted from the $C_2H(\tilde{A},\tilde{B})$ fragments. The assignments of the vibronic bands are given above the corresponding peak profiles. The sharp dips with an asterisk in the lower figure are caused by the intensity drop of the VUV light source associated with the self-absorption of Kr.

B. Origin bands of the $\tilde{D}$ and $\tilde{F}$ states

In the upper panel of Fig. 1, the six vibronic bands, $\tilde{E}$ 3_0^2, $\tilde{D}$ 0_0^0, $\tilde{E}$ 3_0^3, $\tilde{F}$ 0_0^0, $\tilde{E}$ $2_0^1\,3_0^1$, and $\tilde{E}$ 3_0^4, are identified in the increasing order of their band center wave numbers. Among them, the band origin transitions of the $\tilde{D}-\tilde{X}$ and $\tilde{F}-\tilde{X}$ bands appear with the largest intensities at ~74 500 cm^{-1} and ~74 750 cm^{-1}, respectively. In order to derive the bandwidth and the band center wave numbers of these six vibronic bands, the least-squares fit was performed for the spectral shape of the entire region in the upper panel of Fig. 1. In the numerical synthesis of the spectrum, a Lorentzian-type line profile $f_i^L(\nu,\ \nu_i,\ \Gamma_i)$ is adopted for the five transitions and an asymmetric line profile,[16]

$$f_{F0}(\nu,\ \nu_{F0},\Gamma_{F0})=\frac{I_{F0}\left\{q+\left(\frac{2(\nu-\nu_{F0})}{\Gamma_{F0}}\right)\right\}^2}{1+\left\{\frac{2(\nu-\nu_{F0})}{\Gamma_{F0}}\right\}^2}, \tag{2}$$

was adopted for the $\tilde{F}$ 0_0^0 band, where the parameters I_i, ν_i, and Γ_i represent an intensity factor, a band center wave number, and a bandwidth, respectively, and q denotes an asymmetric parameter.[32] The synthesized spectrum,

$$I(\nu)=\sum a_i f_i^L(\nu,\nu_i,\Gamma_i)+b f_{F0}(\nu,\ \nu_{F0},\ \Gamma_{F0}), \tag{3}$$

was fitted to the observed spectrum. The results of the least-squares fit are summarized in Fig. 2 and Table I.

Though the degree of asymmetry for the $\tilde{F}$ 0_0^0 band is small, as represented by the relatively large value of q, q

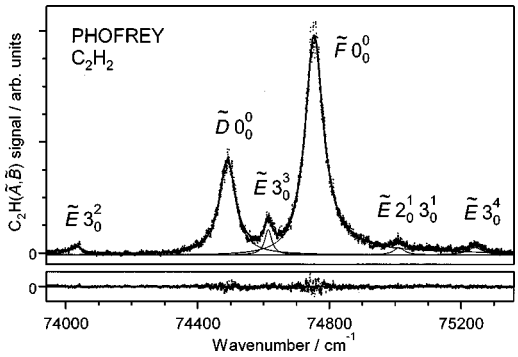

FIG. 2. Comparison of the observed PHOFREY spectrum (dots) in the upper panel of Fig. 1 and the best fit spectrum (bold solid curve) constructed by Lorentzian profiles assigned to the respective six vibronic bands. The Lorentzian components are plotted in a thin solid curve. The residuals of the fit are plotted below the spectrum.

$=21.3(6)$, the inclusion of the q parameter reduced largely the standard deviation of the fit. The FWHMs of the $\tilde{D}-\tilde{X}$ and $\tilde{F}-\tilde{X}$ origin band transitions, $\Gamma(\tilde{D}_0)=58.9(4)$ and $\Gamma(\tilde{F}_0)=66.7(2)$ cm^{-1}, which can be converted, respectively, to the lifetime τ of $\tau=89$ and 79 fs, indicate that the ultrafast dissociation proceeds through these two vibrational levels with comparable rates.

As shown in Table I, the bandwidths of the four $\tilde{E}-\tilde{X}$ transitions are all ~ 40 cm^{-1}, and are much narrower than those of the $\tilde{D}-\tilde{X}$ and $\tilde{F}-\tilde{X}$ transitions (60–180 cm^{-1}), suggesting that the nature of the $\tilde{E}$ state is intrinsically different from the $\tilde{D}$ and $\tilde{F}$ Rydberg states.

TABLE I. Determined term values and bandwidths of the vibronic bands of the $\tilde{D}$, $\tilde{E}$, and $\tilde{F}$ states of acetylene.[a]

State	Assignment	Term value /cm^{-1}	Vibrational term value /cm^{-1}	Width/cm^{-1}
$\tilde{D}$	0	74 490.2(1)	0	58.9(4)
	2^1	76 270[b]	1780	87[b]
	3^1	77 629(3)[c]	3139(3)	184(13)
	$1^1 3^1$	80 677(5)[d]	6187(5)	139(19)
$\tilde{E}$[f]	3^2	74 029(1)	1276	50(4)
	3^3	74 614.5(3)	1861.5	26(1)
	$2^1 3^1$	75 011(1)	2258	40(4)
	3^4	75 243(1)	2490	55(5)
	$2^1 3^2$	75 580[e]	2827	
	3^5	75 850[b]	3097	37[b]
	$2^1 3^3$	76 100[b]	3347	43[b]
$\tilde{F}$	0	74 751.4(1)	0	66.7(2)[g]
	2^1	76 480[b]	1729	53[b]
	3^1	77 817(3)[c]	3066(3)	103(5)
	$1^1 3^1$	80 944(3)[d]	6193(3)	149(14)

[a]The number in parentheses represents a standard deviation (1σ) obtained from the fit.
[b]References 11 and 12.
[c]Calculated from the hot-band transition from the ν_3'' [$=3294.8323(4)$ cm^{-1}] level.
[d]Calculated from the hot-band transition from the $\nu_1''+\nu_3''$ [$=6556.4561(5)$ cm^{-1}] level.
[e]The Lorentzian fit was not performed because of the week intensity.
[f]The origin band wave number, 72 753(10) cm^{-1}, reported in Ref. 14 is adopted to obtain vibrational term values.
[g]The asymmetric parameter was obtained in the fits as $q=21.3(6)$.

C. ν_2' bands of the $\tilde{D}$ and $\tilde{F}$ states

In the lower panel of Fig. 1, the VUV light intensity fluctuates due to the self-absorption of a Kr gas[30] used as a nonlinear medium for the four-wave difference mixing. The effect of the intensity fluctuation can not be canceled out completely even after the intensity normalization procedure, and it causes sharp dips marked by an asterisk in the intensity normalized spectrum. Though the least-squares fit using multiple Lorentzian profiles was not performed for the spectrum in the lower panel, it can be read readily from the spectrum that the widths of the $\tilde{D}\ 2_0^1$ band (~ 80 cm^{-1}) and the $\tilde{F}\ 2_0^1$ band (~ 50 cm^{-1}), are comparable with the those of the $\tilde{D}\ 0_0^0$ and $\tilde{F}\ 0_0^0$ origin bands in the upper panel. These bandwidths obtained here are consistent with the corresponding bandwidths of $\Gamma(\tilde{D}_2)=87$ cm^{-1} and $\Gamma(\tilde{F}_2)=53$ cm^{-1} reported previously by H-atom fragment action spectroscopy.[11,12]

D. ν_3' and $\nu_1'+\nu_3'$ bands of the $\tilde{D}$ and $\tilde{F}$ states

In order to investigate an effect of the antisymmetric CH stretch excitation on the predissociation rate in the $\tilde{D}$ and $\tilde{F}$ states, the IR-VUV double resonance excitation scheme was adopted. Acetylene was excited first to the ν_3'' and $\nu_1''+\nu_3''$ levels in the electronic ground state, and then, it was excited to the corresponding levels in the $\tilde{D}$ and $\tilde{F}$ states by the VUV light,

$$C_2H_2(\tilde{X})+h\nu_{IR}\rightarrow C_2H_2(\tilde{X}\,\nu_3''), \tag{4}$$

$$C_2H_2(\tilde{X}\,\nu_3'')+h\nu_{VUV}\rightarrow C_2H_2(\tilde{D}\,\nu_3',\tilde{F}\,\nu_3'), \tag{5}$$

and

$$C_2H_2(\tilde{X})+h\nu_{IR}\rightarrow C_2H_2(\tilde{X}\,\nu_1''+\nu_3''), \tag{6}$$

$$C_2H_2(\tilde{X}\,\nu_1''+\nu_3'')+h\nu_{VUV}\rightarrow C_2H_2(\tilde{D}\,\nu_1'+\nu_3',\ \tilde{F}\,\nu_1'+\nu_3'). \tag{7}$$

The observed IR-VUV double resonance excitation spectrum is shown in Fig. 3(a). The broad shoulders identified at the positions indicated by an arrow in Figs. 3(b) and 3(c) appeared only when the IR laser light was introduced, and therefore, they were assigned to the double resonance transitions. It is expected that the fundamentals of the C–H antisymmetric stretch (ν_3') of the $\tilde{D}$ and $\tilde{F}$ states are also close to $\nu_3''=3294.8$ cm^{-1} of the electronic ground state, and that the 3_1^1 bands of the $\tilde{D}-\tilde{X}$ and $\tilde{F}-\tilde{X}$ transitions should appear near their electronic band origin transitions. Therefore, the broad bands located at $\sim 74\,300$ and $\sim 74\,500$ cm^{-1} in Fig. 3(b) were assigned to the $\tilde{F}\ 3_1^1$ and $\tilde{D}\ 3_1^1$, respectively.

Since these 3_1^1 bands of the $\tilde{D}$ and $\tilde{F}$ states are shifted by about 200 cm^{-1} to the lower wave number side from the respective electronic origins, the $1_1^1\,3_1^1$ bands are expected to be shifted further by 200 cm^{-1}. Consequently, the broad

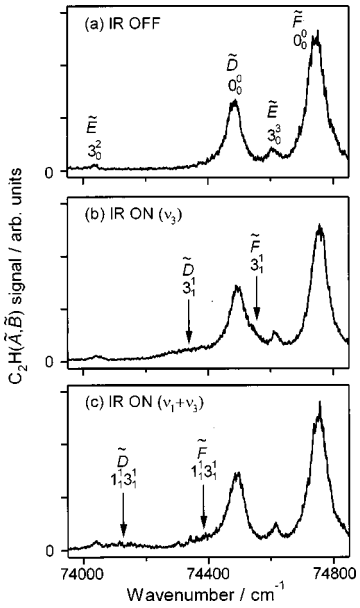

FIG. 3. The PHOFREY spectra of C_2H_2 in the 73 950–74 850 cm^{-1} range recorded by monitoring fluorescence emitted from $C_2H(\tilde{A},\tilde{B})$ fragments; (a) the one-photon PHOFREY spectrum, (b) the IR-VUV DR PHOFREY spectrum observed when the IR laser is tuned to the $P(3)$ line of the ν_3'' vibrational transition at 3287.7 cm^{-1}, and (c) the IR-VUV DR PHOFREY spectrum observed when the IR laser is tuned to the $P(3)$ line of the $\nu_1''+\nu_3''$ vibrational transition at 6549.3 cm^{-1}.

bands located at ~74 100 and ~74 400 cm^{-1} in Fig. 3(c) were assigned to $\tilde{D}\ 1_1^1\ 3_1^1$ and $\tilde{F}\ 1_1^1\ 3_1^1$, respectively.

In order to confirm that these new bands are double resonance transitions, the IR laser wavelength was scanned in the narrow wavelength range around the centers of the ν_3'' and $\nu_1''+\nu_3''$ band, while fixing the VUV wavelength at the double resonance (DR) peak. In addition, photoacoustic (PA) spectrum of acetylene was measured simultaneously to assign the rotational transitions appearing in the DR-IR excitation spectrum. The two kinds of IR excitation spectra obtained for the ν_3 transition are shown in Fig. 4. They are (i) the DR-IR

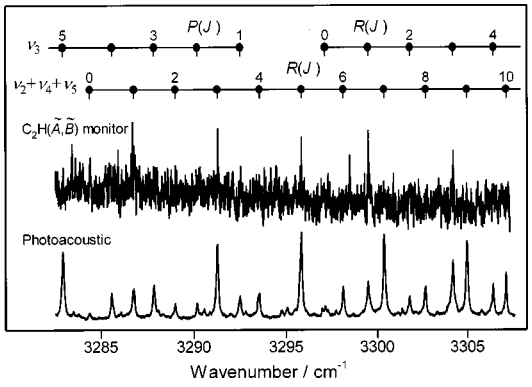

FIG. 4. The IR-VUV double resonance excitation spectrum of C_2H_2 (upper) obtained by scanning the IR-laser wave number while monitoring the fluorescence emitted from the $C_2H(\tilde{A},\tilde{B})$ fragments. The VUV laser wave number is tuned to 74 522 cm^{-1}, where the $\tilde{F}-\tilde{X}\ 3_1^1$ band is located. The photoacoustic (PA) excitation spectrum in the IR range (lower) observed simultaneously is compared. As shown in the rotational assignments, the two vibrational bands, i.e., ν_3'' and $\nu_2''+\nu_4''+\nu_5''$, overlap with each other in this IR range.

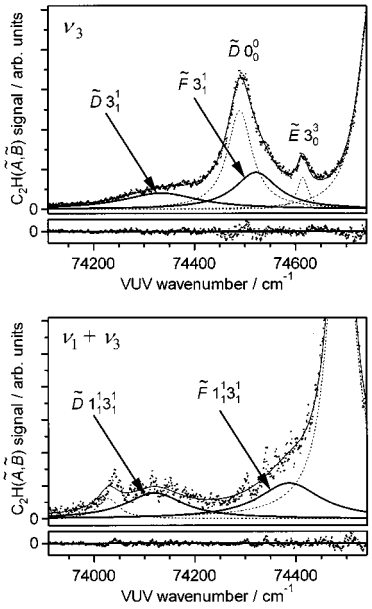

FIG. 5. The results of the fits of the IR-VUV DR PHOFREY spectra obtained when the IR wave number is tuned to the $P(3)$ line of the ν_3'' (upper) and $\nu_1''+\nu_3''$ (lower) bands. The observed spectrum is drawn in dots and the best-fit spectrum is drawn in a thin solid curve. The components of the double-resonance bands, i.e., $\tilde{D}3_1^1$ and $\tilde{F}3_1^1$ in the lower panel and $\tilde{D}1_1^1 3_1^1$ and $\tilde{F}1_1^1 3_1^1$ in the upper panel are drawn in bold solid curves. The other components, i.e., the one-photon excitation components, are drawn in broken curves. The residuals of the fit are plotted below the respective spectra.

excitation spectrum obtained by monitoring the total fluorescence emitted from the $\tilde{A}$ and $\tilde{B}$ states of the C_2H photofragments (upper trace) and (ii) the PA-IR excitation spectrum (lower trace).

In the IR wave number range in Fig. 4, two rotational band origins for the vibrational transition to the ν_3'' level, 3294.8323(4) cm^{-1}, and that to the $\nu_2''+\nu_4''+\nu_5''$ level, 3281.8934(3) cm^{-1}, are located. These two levels interact with each other through the 3/245 Fermi resonance.[33] The rotational assignments for the ν_3'' and $\nu_2''+\nu_4''+\nu_5''$ bands are shown just above the DR-IR excitation spectrum. Though the PA-IR excitation spectrum exibits a pressure broadening, the wave number positions of the sharp peaks ($J\leqslant 5$) in the DR-IR excitation spectrum measured under jet-cooled conditions are in good agreement with the centers of the rovibrational peaks in the PA-IR excitation spectrum. On the basis of this frequency match of the rotational transitions, the fluorescence peaks in the upper trace of Fig. 4 and the shoulder appearing at 74 500 cm^{-1} in Fig. 3(b) were assigned unambiguously to the IR-VUV DR transition, i.e., the $\tilde{F}\ 3_1^1$ band.

The least-squares fit was performed for the observed peak profiles in the IR-VUV DR PHOFREY spectra in Figs. 3(b) and 3(c). In Fig. 5, the observed and best-fit convoluted spectra are shown with the Lorentzian components for the $\tilde{D}\ 1_1^1\ 3_1^1$ and $\tilde{F}\ 1_1^1\ 3_1^1$ bands in the upper panel and those for the $\tilde{D}\ 3_1^1$ and $\tilde{F}\ 3_1^1$ bands in the lower panel. In the least-squares fit, the band-center wave numbers and bandwidths of the respective one-photon excitation bands, which overlap

with these double resonance bands, were fixed to the same values as those determined in Sec. III B.

From the least-squares fit, the FWHMs of the $\tilde{D}\,3_1^1$, $\tilde{F}\,3_1^1$, $\tilde{D}\,1_1^1\,3_1^1$, and $\tilde{F}\,1_1^1\,3_1^1$ bands were determined to be $\Gamma(\tilde{D}_3)=184(13)$, $\Gamma(\tilde{F}_3)=103(5)$, $\Gamma(\tilde{D}_{13})=139(19)$, and $\Gamma(\tilde{F}_{13})=149(14)$ cm^{-1}, respectively. This significant broadening identified for all the ν_3' excited levels suggests that the ν_3' mode accelerates the rate of dissociation through the $\tilde{D}$ and $\tilde{F}$ states to a large extent. In the $\tilde{F}$ state, the additional excitation in the ν_1' mode increased further the dissociation rate, i.e., $\Gamma(\tilde{F}_0)<\Gamma(\tilde{F}_3)<\Gamma(\tilde{F}_{13})$, while in the $\tilde{D}$ state, the additional ν_1' excitation effected in a different way, i.e., $\Gamma(\tilde{D}_0)<\Gamma(\tilde{D}_{13})<\Gamma(\tilde{D}_3)$.

E. Mechanism of the C_2H ($\tilde{A},\tilde{B}$) formation

Herman and Colin measured an absorption spectrum of the $\tilde{D}-\tilde{X}$ and $\tilde{F}-\tilde{X}$ transitions under bulk conditions. From their absorption spectrum, the ratio $R=I(\tilde{D})/I(\tilde{F})$ of the spectral intensities, $I(\tilde{D})$ and $I(\tilde{F})$, of the $\tilde{D}-\tilde{X}$ and $\tilde{F}-\tilde{X}$ origin-band transitions were estimated to be $R\sim0.17(2)$. In contrast, the intensity ratio is $R=0.4(1)$ in our PHOFREY spectrum shown in the upper panel of Fig. 1, indicating that the quantum yield of $C_2H(\tilde{A},\tilde{B})$ from the vibrational ground state of the $\tilde{D}$ state is larger than that from the vibrational ground state of the $\tilde{F}$ state by a factor of 2.4.

Löffler *et al.*[11,12] measured one-photon VUV excitation spectra of jet-cooled acetylene in the 75 600–76 600 cm^{-1} region by the H-atom fragment action spectroscopy. The intensity of the $\tilde{F}\,2_0^1$ band was 1.5 times as large as that of the $\tilde{D}\,2_0^1$ band in their spectrum, while the $\tilde{F}\,2_0^1$ band is slightly weaker than the $\tilde{D}\,2_0^1$ band in our PHOFREY spectrum in the lower panel of Fig. 1. Because the dissociation rate in this energy region is much faster than a radiative relaxation rate, and only minor contribution is expected from the elimination of a molecular hydrogen,[7,34] the quantum yield of the H-atom production is considered to be unity. Therefore, the differences above indicate that the quantum yield of the $C_2H(\tilde{A},\tilde{B})$ production is larger in the ν_2' excited state of the $\tilde{D}$ state than in the ν_2' excited state of the $\tilde{F}$ state.

The preference of the $C_2H(\tilde{A},\tilde{B})$ formation in the $\tilde{D}$ state compared with the $\tilde{F}$ state identified both in the origin and 2_0^1 bands may be ascribed to the Π electronic character of the $\tilde{D}$ state. Because the potential energy surfaces which lead to the fragmentation into $C_2H(\tilde{A},\tilde{B})$ are known to have a Π character,[19] the dissociation through the $\tilde{D}$ state having the same Π character would be preferred to that through the $\tilde{F}$ state having a Σ electronic character.

In Fig. 6, the bandwidths of the observed peaks in the PHOFREY spectra listed in Table I are plotted as a function of their term values. Since the ν_3' coordinate corresponds with the dissociation coordinate in the linear geometry, the bandwidth broadening associated with the ν_3' excitation could be ascribed to a larger overlap between the vibrational wave functions of the ν_3' excitated levels in the $\tilde{D}$ and $\tilde{F}$ Rydberg states and the continuum wavefunction of a repulsive state leading to the C_2H+H dissociation. The different behavior of the dissociation rate in the $\tilde{D}$ and $\tilde{F}$ states identified when ν_1 is excited in addition to ν_3, $\Gamma(\tilde{D}_3)>\Gamma(\tilde{D}_{13})$, and $\Gamma(\tilde{F}_3)<\Gamma(\tilde{F}_{13})$, may indicate that the simultaneous excitation of the ν_1 and ν_3 modes enhances the wave function overlap with the continuum state in the $\tilde{F}$ state, while it reduces the overlap in the $\tilde{D}$ state.

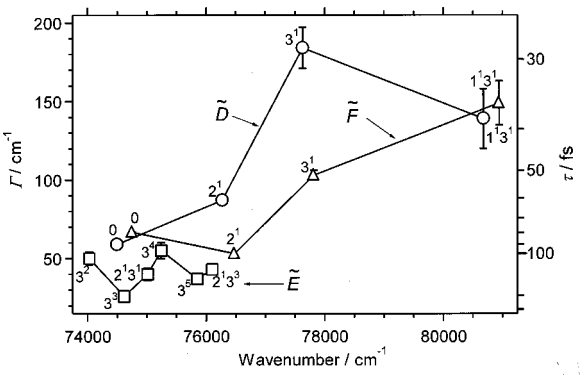

FIG. 6. The bandwidths, Γ, for the vibrational levels of the $\tilde{D}$ (○), $\tilde{E}$ (□), and $\tilde{F}$ (△) states of C_2H_2 listed in Table I as a function of the term value. The ordinate on the right-hand side represents the lifetime, τ, converted from Γ using $\tau\cdot\Gamma=5.3$ ps cm^{-1}. The length of the vertical bars represents an estimated limit of uncertainties.

The bandwidths for the transition to the $\tilde{E}$ state levels ($\Gamma\sim40$ cm^{-1}) are much narrower than those for the $\tilde{D}$ and $\tilde{F}$ states ($\Gamma=60$–180 cm^{-1}). This means that the dissociation proceeds much slower in the $\tilde{E}$ state. Since the equilibrium geometry of the $\tilde{E}$ state is considered to be displaced from the planar configuration, the slow dissociation rate in the $\tilde{E}$ state implies that dissociative wave functions on the continuum state have a probability distribution considerably displaced from the $\tilde{E}$ state geometry, i.e., the dissociation may proceed from planar or linear geometry.

On the basis of the H-atom fragment action spectroscopy of acetylene, Löffler *et al.*[12] suggested the existence of the statistical predissociation pathways from the $\tilde{D}$, $\tilde{E}$, and $\tilde{F}$ states, which produce $C_2H(\tilde{A})$ photofragments via mixing with the $\tilde{A}$ or $\tilde{B}$ state. When the dissociation from the $\tilde{D}$, $\tilde{E}$, and $\tilde{F}$ manifolds proceeds through such a common intermediate state, the relative yields of $C_2H(\tilde{A}$ or $\tilde{B})$ for these electronic states are expected to be almost the same. Therefore, the clear dependences of the C_2H yields on the initially excited electronic state as well as on their vibrational states identified in the present study indicate that the memory of the electronic and vibrational characters of the initially prepared state is preserved persistently in the course of the photodissociation.

IV. SUMMARY

The $\tilde{D}\,^1\Pi_u$ and $\tilde{F}\,^1\Sigma_u^+$ Rydberg states and the $\tilde{E}\,^1A$ valence state of jet-cooled C_2H_2 located in the 135.3–130.8 nm region were investigated by measuring excitation spectra

called VUV photofragment yield (PHOFREY) spectra and IR-VUV double resonance PHOFREY spectra, in which visible emission from the $C_2H(\tilde{A},\tilde{B})$ photofragments was monitored. The term values and homogeneous bandwidths of the vibrational levels in the three overlapping electronic states were determined with high-precision from least-squares fits to the observed peaks profiles broadened by a fast dissociation process.

Among the new spectroscopic findings, the observation of the transitions of $\tilde{D}\ 3_1^1$, $\tilde{D}\ 1_1^1\ 3_1^1$, $\tilde{F}\ 3_1^1$, and $\tilde{F}\ 1_1^1\ 3_1^1$ are noteworthy. Their vibrational assignments were confined by scanning the IR wavelength in the IR-VUV DR measurements. It should be mentioned also that the present measurements under jet-cooled conditions enabled us to assign securely the relatively weak $n\nu_3'$ $(n=2-5)$ and $\nu_2'+n\nu_3'$ $(n=1-3)$ progressions of the $\tilde{E}-\tilde{X}$ transition.

Regarding the photodissociation rate, it was found that the $\tilde{D}$ and $\tilde{F}$ Rydberg states behaved in a similar manner, i.e., the lifetime broadening of the origin bands for the $\tilde{D}$ and $\tilde{F}$ states were 58.9 and 66.7 cm^{-1}, respectively, and the peak-width became approximately twice as large as that for the origin bands once the C–H antisymmetric stretch was excited. However, the quantum yield for the production of $C_2H(\tilde{A},\tilde{B})$ fragment through the 0^0 and 2^1 levels of the $\tilde{D}$ Rydberg state was approximately twice as larger as that through the corresponding levels of the $\tilde{F}$ Rydberg state. On the other hand, the broadened widths for the $\tilde{E}$ state levels were in the range of 26–50 cm^{-1}, and no clear dependence on the vibrational mode was identified.

ACKNOWLEDGMENTS

The authors thank Dr. A. Hishikawa, Dr. A. Iwamae, and Dr. A. Iwasaki for their helpful discussions and experimental assistance. The present work has been supported by the CREST (Core Research for Evolutionary Science and Technology) fund from Japan Science and Technology Corporation.

[1] M. Suto and L. C. Lee, J. Chem. Phys. **80**, 4824 (1984).
[2] W. C. Price, Phys. Rev. **47**, 444 (1935).
[3] P. G. Wilkinson, J. Mol. Spectrosc. **2**, 387 (1958).
[4] M. Jungen, Chem. Phys. **2**, 367 (1973).
[5] W. E. Kammer, Chem. Phys. **5**, 408 (1974).
[6] M. Herman and R. Colin, J. Mol. Spectrosc. **85**, 449 (1981).
[7] H. Okabe, J. Chem. Phys. **78**, 1312 (1983).
[8] M. Peric, R. J. Bunker, and S. D. Peyerimhoff, Mol. Phys. **53**, 1177 (1984).
[9] M. Peric, S. D. Peyerimhoff, and R. J. Bunker, Mol. Phys. **55**, 1129 (1985).
[10] J. K. Lundberg, D. M. Jonas, B. Rajaram, Y. Chen, and R. W. Field, J. Chem. Phys. **97**, 7180 (1992).
[11] P. Löffler, D. Lacombe, A. Ross, E. Wrede, L. Schnieder, and K. H. Welge, Chem. Phys. Lett. **252**, 304 (1996).
[12] P. Löffler, E. Wrede, L. Schnieder, J. B. Halpern, W. M. Jackson, and K. H. Welge, J. Chem. Phys. **109**, 5231 (1998).
[13] T. M. Orland, S. L. Anderson, J. R. Appling, and M. G. White, J. Chem. Phys. **87**, 852 (1987).
[14] M. N. R. Ashfold, B. Tutcher, B. Yang, Z. K. Jin, and S. L. Anderson, J. Chem. Phys. **87**, 5105 (1987).
[15] M. Takahashi, M. Fujii, and M. Ito, J. Chem. Phys. **96**, 6486 (1992).
[16] K. Tsuji, N. Arakawa, A. Kawai, and K. Shibuya, J. Phys. Chem. **106**, 747 (2002).
[17] A. Hishikawa, K. Ohde, R. Itakura, S. Liu, K. Yamanouchi, and K. Yamashita, J. Phys. Chem. A **101**, 694 (1997).
[18] W. R. M. Graham, K. I. Dismuke, and W. Weltner, J. Chem. Phys. **60**, 3817 (1974).
[19] H. Okabe, J. Chem. Phys. **62**, 2782 (1975).
[20] S.-K. Shin, S. D. Peyerimhoff, and R. J. Buenker, J. Mol. Spectrosc. **74**, 124 (1979).
[21] Y. Saito, T. Hikida, T. Ichimura, and Y. Mori, J. Chem. Phys. **80**, 31 (1984).
[22] R. K. Sander, J. J. Tiee, C. R. Quick, R. J. Romero, and R. Ester, J. Chem. Phys. **89**, 3495 (1988).
[23] Y.-C. Hsu, Y.-J. Shiu, and C.-M. Lin, J. Chem. Phys. **103**, 5919 (1995).
[24] A. Campos, S. Boye, Ph. Brechignac, S. Douin, C. Fellows, N. Shafizadeh, and D. Gauyacq, Chem. Phys. Lett. **314**, 91 (1999).
[25] M. Boggio-Pasqua, Ph. Halvick, M.-T. Rayez, J.-C. Rayez, and J.-M. Robbe, J. Phys. Chem. A **102**, 2009 (1998).
[26] A. Bergeat, T. Calvo, G. Dorthe, and J.-C. Loison, J. Phys. Chem. A **103**, 6360 (1999).
[27] J. Zhang, C. W. Riehn, M. Dulligan, and C. Wittig, J. Chem. Phys. **103**, 6815 (1995).
[28] R. P. Schmid, T. Arusi-Parpar, R. J. Li, I. Bar, and S. Rosenwaks, J. Chem. Phys. **107**, 385 (1997).
[29] R. P. Schmid, Y. Ganot, I. Bar, and S. Rosenwaks, J. Chem. Phys. **109**, 8959 (1998).
[30] K. Yamanouchi and S. Tsuchiya, J. Phys. B **28**, 133 (1995).
[31] K. Hoshina, A. Iwasaki, K. Yamanouchi, M. P. Jacobson, and R. W. Field, J. Chem. Phys. **114**, 7424 (2001).
[32] U. Fano, Phys. Rev. **124**, 1866 (1961).
[33] B. C. Smith and J. S. Winn, J. Chem. Phys. **89**, 4638 (1988).
[34] A. M. Wodtke and Y. T. Lee, J. Phys. Chem. **89**, 4744 (1985).